Mechanics Research Communications 137 (2024) 104261

Contents lists available at ScienceDirect

Mechanics Research Communications

journal homepage: www.elsevier.com/locate/mechrescom

Evidence of nonlinearity tailoring in static and dynamic responses of honeycomb and auxetic hourglass lattice metastructures

Vivek Gupta [a], Sondipon Adhikari [b], Bishakh Bhattacharya [a,*]

[a] Department of Mechanical Engineering, Indian Institute of Technology Kanpur, India
[b] The University of Glasgow, Glasgow, United Kingdom

ARTICLE INFO

Keywords:
Hourglass
Frequency response
Auxetic
Honeycomb
Nonlinear
Phase-portraits

ABSTRACT

Nature's morphology and optimal energetic solutions remain the key motivation for designing cellular-based lattice structures. Understanding the nonlinear dynamical behaviors that arise from different lattice topologies of such structures in the metastructure framework is crucial for their successful implementation in various novel designs and technologies related to vibration and shape control. This paper presents a study of the static and dynamic response of auxetic and honeycomb lattices with hourglass or dome-shaped metastructures. The potential tailoring of nonlinearity of such responses through various design parameters that play a vital role in shaping the dynamic properties of such structures is discussed here. The impact of cell design parameters on the resulting macroscopic behavior is assessed using both numerical simulations and experimental studies. The transition from softening to hardening nonlinear dynamic responses is reported with cell topologies ranging from the regular honeycomb to auxetic topologies that are widely used as fundamental cells of cellular materials design. The experimental study is based on the time responses measured to verify the numerical predictions. The experimental system consists of different 3D printed hourglass samples based on the auxetic and honeycomb lattices on which dynamic testing using a laser Doppler vibrometer is performed. The design strategies proposed in this paper can be integrated into a wide range of lattice-based materials for noise and vibration control applications and biomedical devices.

1. Introduction

The exploration of mechanical metamaterials motivated the scientific community to study the dynamics of lattice topologies in the broader sense. These metamaterials belong to the class of designer materials whose unique tailor-made properties originate from their designs at a smaller scale [1–4] such as metastructures. One of the unconventional properties of a metastructure is the possibility to tune the Poisson's ratio through the variation in micro-structural designs. The materials with negative (called auxetics) and zero values of the Poisson's ratio (ZPR) are often studied due to their interesting properties and functionalities honed for wide range of applications [5,6].

Extreme engineering applications are becoming ever more demanding in many sectors of the industry today. High-performance materials are necessary for a range of devices, including professional apparel, naval, aerospace, civil structures, and implants for surgical use. Traditional materials can no longer keep up with this ever-increasing demand for performances, and consequently, materials exhibiting new exotic behaviors are designed. The cellular architected materials have shown enhanced structural properties as well as the ability to control elastic wave propagation [7–9], making them ideal for multifunctional applications. These structures are acquired many advantages in terms of high strength-to-weight ratio, excellent energy absorption, and minimizing material requirements [10]. All the major industries have been exploiting the benefits of such structures due to their prevalence over a wide band of excitation frequency. On the other hand, the emergence of additive manufacturing technologies enables fabrication of cellular materials with more complex architectures, and many novel architected materials have been created over the last few years. It enables the development of arbitrary complex geometry based on lattice topologies [11–15], woven topologies [16], hierarchical structures [17–19], honeycomb structures [11,20–22], bio-inspired cellular materials [23] and foam-like metamaterials [24] and therefore provides an excellent opportunity to explore new mechanical metamaterials. Honeycomb and auxetic [25,26]-based cellular lattice structures with various shapes and designs are of particular interest to engineers, primarily because of their high bending stiffness to weight ratio [27], energy absorption [28–30], wave propagation [7,8], and relative ease of manufacturing due to their intrinsic periodicity. The dynamic characteristics of these lattices have

* Corresponding author.
E-mail addresses: vivekgup@iitk.ac.in (V. Gupta), Sondipon.Adhikari@glasgow.ac.uk (S. Adhikari), bishakh@iitk.ac.in (B. Bhattacharya).

https://doi.org/10.1016/j.mechrescom.2024.104261
Received 24 January 2024; Received in revised form 27 February 2024; Accepted 4 March 2024
Available online 14 March 2024

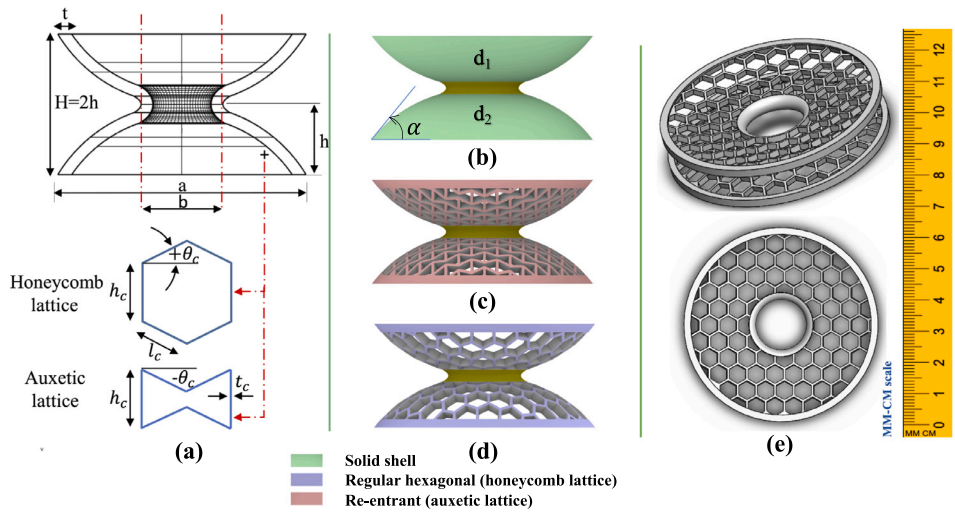

Fig. 1. The proposed hourglass-shaped lattice metastructure and its geometric specifications are labeled in diagram (a). It is a combination of two domes $d1$ and $d2$ joined by G1 spline surface to avoid stress concentration, (b, c, d) named as homogeneous (having symmetrical lattice domes) categories. (a) Schematic of an hourglass shape lattice with standard representative cells such as honeycomb and auxetic with the included angle, cell height, and cell beam thickness is θ_c, h_c and t_c, are shown respectively. The overall height of the hourglass, inner and outer diameter is H, b, and a, respectively. (b) Homogeneous categories of hourglass as a solid shell (H:SS), (c) with auxetic lattices (H:AA), (d) with regular honeycomb lattices (H:HH). (e) An isometric and top view of the model with a different height (H) is shown along with the $mm-cm$ scale.

been significantly investigated within the structural dynamics research and development community in the last four decades. Numerous regular shapes such as planer [31], tubular [32] and cubic geometries [33] that are relatively simpler to fabricate are reported in the literature exhaustively. However, all these lattice metastructures have a limited scope of tunability due to their relatively simpler shapes. Hence, broadband design of the metastructures require novel unit cells with more customizable structural properties such as stiffness and compliance.

Nonlinearities play a tremendous role in engineering and can be tailored by the metamaterial unit cell geometry. Good effort has been made to explore the tuneable response mechanical behavior by altering topologies or geometries of lattice structures. For example, Kang et al. [34], shows geometrical frustration induced by buckling in continuum triangular cellular structures. They specifically discussed the porosity of the system controls the appearance of a specific configuration. Wang et al. [35] intentionally exploited buckling is as a novel and practical approach to control the propagation of elastic waves in order to design tunable acoustic metamaterials and accounted the effect of nonlinear pre-deformation. Furthermore, the non-linear response of pore structures and instabilities is utilized to design a novel class of responsive behavior [36]. Though this work was limited to 2D, circular, and elliptical pores. Milton et al. [37] discussed possible deformation of nonlinear unimode metamaterials constructed from rigid bars and pivots. They show the explicit construction of any continuous trajectory is achievable to a high degree of approximation. The structures considered here are difficult to build practically because of their multiscale nature and theoretical assumptions of rigid bars and pivots. The aforementioned research has yet to specifically discuss the type of nonlinearity or the tailoring of nonlinear behavior of lattice through its constitutive cells and lags of experimental validations. This work fills the research gaps to utilize the instabilities of lattice metamaterials to produce different types of controlled nonlinearities using dome-shell lattice, mainly based on the most generalized cells known as honeycombs and auxetic. Its experimental validation on dynamic responses covers transitions from softening to hardening stiffness profiles, makes it practically realizable. This study presents the conceptual model along with a fabricated metastructure developed using additive manufacturing technology. Numerical simulation, additive layer manufacturing (3D printing), and experimental testing are carried out to evaluate the mechanics of the system and reveal the underlying physics responsible for their unusual nonlinear behavior. It is observed from the existing literature that the dome based lattice structures have rarely been explored in metastructure design, even though such structures have found good potential in tuning the stiffness and Poisson's ratio [38]. We have expanded the design space of metastructure by integrating the advantage of different lattice geometry with the enhanced tunability of the hourglass shape. The shape of the hourglass structure is in itself an exciting design that contains a combination of two oppositely oriented coaxial domes. This configuration enables us to integrate standard lattices based on auxetic and regular honeycomb as shown in Fig. 1.

2. Modeling and simulations of the nonlinear hourglass lattice

In the present study, the static structural analysis has been performed using the finite element analysis (FEA) package Ansys 15.0, as shown in Fig. 2. The modeling of hourglass samples is carried out in SolidWorks and imported to Ansys workbench. The static structural analysis for the large deflections has been performed to account for the nonlinear structural effects that arise due to curvature and lattice topologies. Small load steps are essential for the accurate calculation of the snap-through phenomenon in nonlinear analysis and for the convergence of the solution. The substeps analysis is defined by 20 initial substeps with a minimum of 20 and a maximum of 100 steps in the subspace solver, which is preferable to deal with complex geometries. For this nonlinear geometric analysis, the force convergence criterion has been observed to achieve the actual forces in the system. The number of equilibrium iterations for each subsequent substeps has been closely measured in the given time intervals. Here, we have used stabilization techniques for getting stability in nonlinear convergence. It allows for simulating instability with Newton–Raphson method which arises in case of converging rigid body motions caused by snap-through of the hourglass model. The constant stabilization has been performed in a nonlinear control environment with the energy dissipation ratio 0.1 activated from the first substep and force limit 0.2. The base rib of the hourglass is provided a zero displacement constraint to the z-axis under the displacement boundary condition. The ramp loading are 100 N, 700 N, 76 N along $-z$-axis applied to the top surface of honeycomb, solid shell, and auxetic type hourglass samples, respectively, depending upon failure criterion. The load–deflection curves were obtained using a deformation probe along z-direction pivoting to the top edge. The nonlinear (NL) softening effect was observed in the auxetic-based sample and the NL hardening effect in the honeycomb sample. The

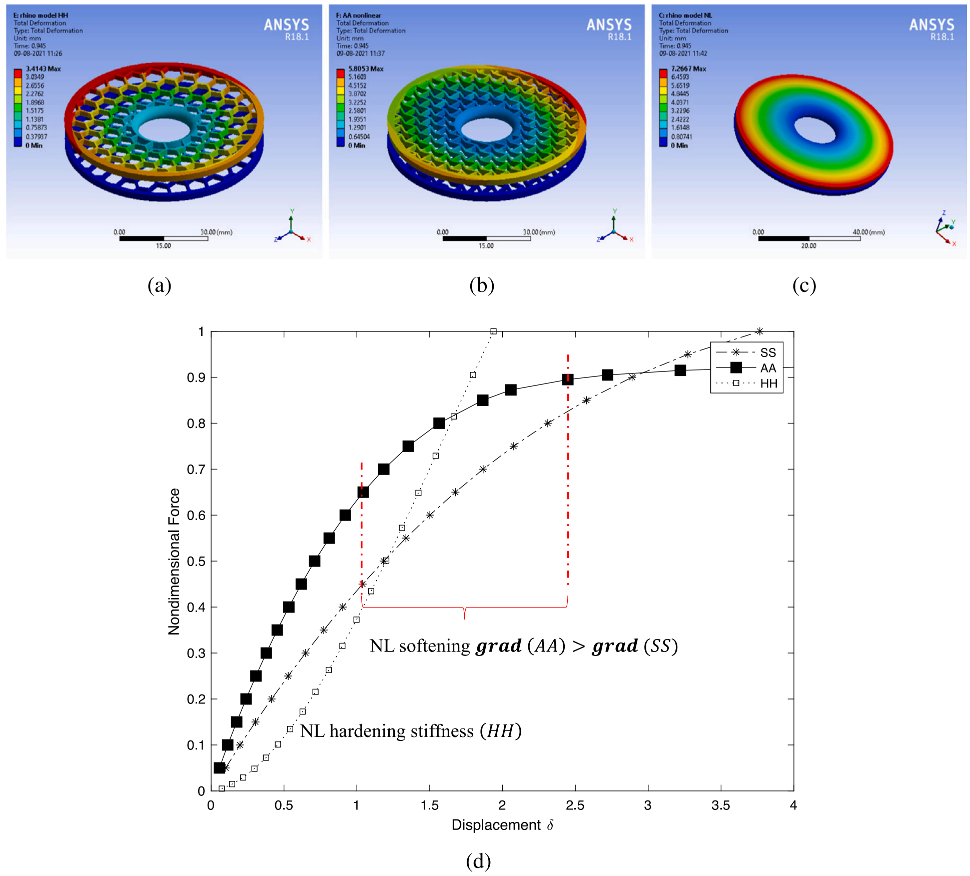

Fig. 2. Numerical simulation results of static structural analysis for three different kinds of lattice metastructure (structural nonlinearity taken into account) have been shown. (a) for honeycomb, (b) auxetic, and (c) solid cells, respectively. (d) Plots of resultant nondimensional force deflections profiles with the observation of varying nonlinearity has been shown for different class of subjects.

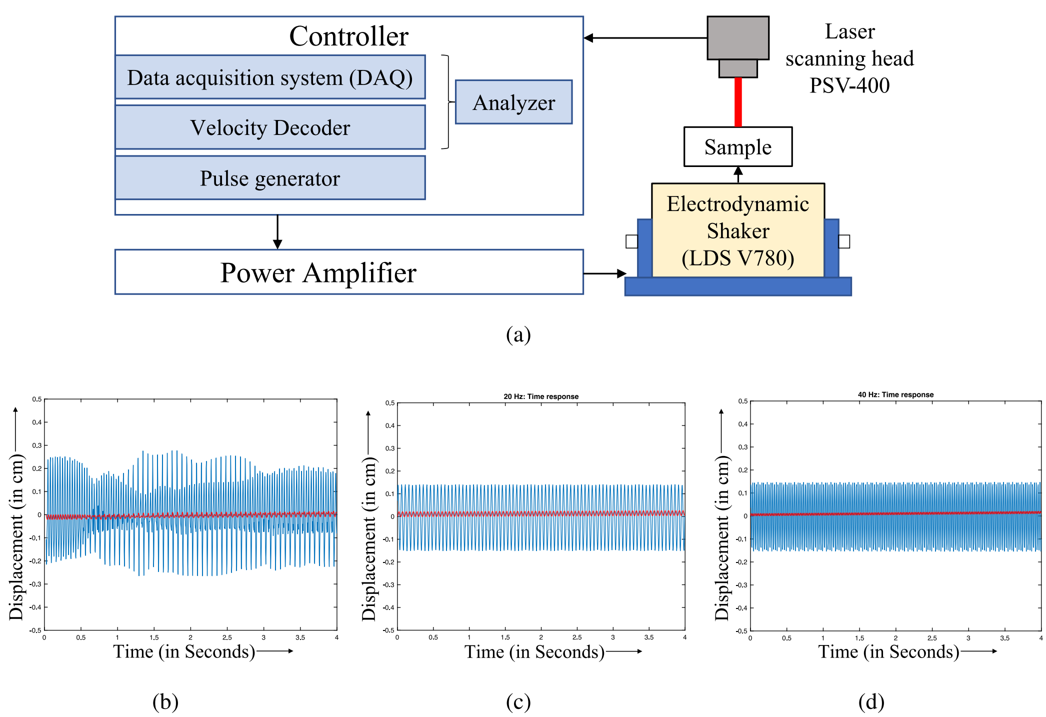

Fig. 3. (a) Schematic diagram of scanning laser Doppler vibrometer and its associated modules consists of controller, power amplifier, electrodynamic shaker and laser scanning head of LDV. (b, c, d) Time domain response captured near the resonating frequencies of different 3D printed hourglass samples with h/t ratio is 4.

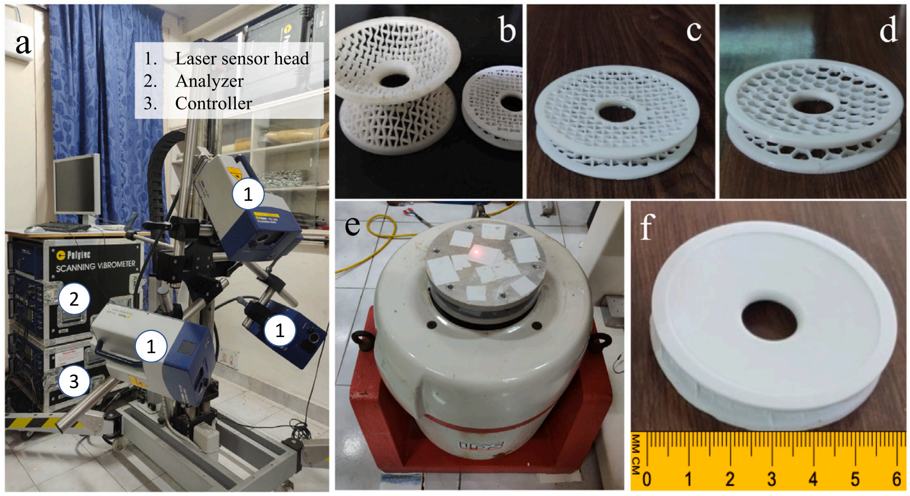

Fig. 4. Experimental setup and sample preparations: (a, e) Shows elements of LDV and sample attachments with electrodynamic shaker. (b, c, d, f) 3D printed hourglass samples of three fundamental cellular configurations with h/t ratio is 4. It is observed from the previous research the h/t ratio equals to $2\sqrt{2}$ gives high zero rate stiffness profiles. The immediate higher h/t ratio between $2\sqrt{2}$ to 5 gives nonlinear stiffness profiles.

nonlinear softening gradient in the auxetic (AA) sample is found to be quite higher than the solid shell (SS) at a higher displacement range, as shown in Fig. 2d.

In the previously published studies [38,39], we had discussed the static mechanical response of the designed metamaterial that shows the combinations of different types of nonlinear stiffness profiles depending upon (h/t) ratios. Therefore, to analyze the acoustic properties of the designed periodic hourglass structure, the phononic band structure and transmission spectrum are determined for the metamaterial with specific structural parameters. The designed hourglass metastructure with the constituent lattice of regular honeycomb and auxetic structure has shown the dependencies of its dynamics to the lattice geometry. In this study, the experimental studies have been performed to quantify the softening and hardening response and its lattice dependencies. The 3D printing material PLA (polyactic acid thermoplastics) provided by Taulman 3D is used to print hourglass metastructure as an experimental sample. The basic properties of PLA material are characterized by Young's modulus of (E) 3.5 GPa, Poisson's ratio (ν) 0.3, and density (ρ) 1.25 $\mathrm{gm/cm^3}$. The modeling of 3D printed samples ($d1$ and $d2$ domes with symmetrical lattice) have been fabricated using Ultimaker 3.0 Extended multi-material 3D printer. The developed metastructure samples are manufactured as a single body with $d1$ and $d2$ domes joined by a smooth spline surface to avoid the stress concentration. The domes are constituted with standard lattices, i.e. auxetic, regular honeycomb, and solid shell. The spherical diameter of $d1$ and $d2$ domes are 245 mm, hourglass height (H) is 8.5 mm (that makes the undeformed height of each dome h =4.25 mm), radial thickness 2 mm with the outer base diameter (d_o) is 64 mm, and internal (d_i) 21 mm. The lattice beam thickness is 0.5 mm with the internal angle (θ_c) for regular honeycomb as 60°, and included internal angle $(-\theta_c)$ for auxetic (re-entrant type) to be −35°. The additive manufacturing specifications are used for fabrication of the samples shown in Table 1. The slicing was performed in Cura version 4.5 with layer height thickness of 0.12 mm, 100% infill density with triangular infill pattern. Rectilinear, and zig-zag supports (minimum 45-°overhang angle) were used to prevent the sample from collapsing. All the samples were printed in the same layer orientation to maintain uniform mechanical properties considered under dynamic testing.

To analyze the dynamics of the samples, non-contact vibration measurement tests were conducted using a laser-based scanning method to capture the vibrating surfaces. The schematic diagram of the scanning laser Doppler vibrometer, along with its associated modules, can be seen in Fig. 3. The steady-state time-domain response was recorded in the vicinity of the resonating frequencies for various 3D printed hourglass samples with an h/t ratio of 4. The collected average amplitude data of the displacement of the top plate was plotted against the corresponding frequency values to generate the forward response curves. A 3D laser Doppler vibrometer (LDV) from Polytec, mounted on a tripod, is used to measure velocity signals along the beam. The NI-DAQ systems are used for data acquisition and sample processing. Each setup consists of a base and top aluminium plate (weighing 200 g) under which hourglass samples are sandwiched. A retro-reflective tape is applied to the top surface of dead mass (centrally) and bottom base plate (which is used to couple exciter with the hourglass sample in the z-direction), enhancing its ability to reflect the incident laser beam, as shown in Fig. 4. The sinusoidal wave is generated by the exciter (LDS-electrodynamic shaker V780) in the z-direction. The discreet frequency responses at every 10 Hz of increments of the top and bottom plate are measured using laser sensors 1 and 2, respectively. The average of peak to peak signal values of the displacement along the z-direction of the incident plane (base plate) and exit plane (dead mass or top plate) is measured through the signal processing tool in MATLAB. The frequency response function (FRF) data up to 500 Hz were analyzed under different gains.

3. Results of simulations and experiments

It has been found in the literature that the dome shells give nonlinear stiffness profiles inherently due to their geometrical shape if compressed along the longitudinal axis [38]. But that happens for homogeneous materials with a positive Poisson ratio. The novelty of the tuning nonlinear stiffness response comes from auxetic lattices that are well known for negative Poisson's ratio forms synclastic curvature that is in accord with the dome curvature and honeycomb's anticlastic curvature. These cellular cuts not only give more customizability to the hourglass but also reduce instabilities coming due to the snap-through phenomenon; in turn, it gives more controlled stiffness to the transition region that passes from one equilibrium state to another. Detecting bifurcation points that depend upon lattice geometry has been explored to quantify the sensitivity of the hourglass oscillator. The observation of the sudden jump in the displacement amplitude by operating it near resonance frequency signifies the snap-through-like behavior of the dome shells of the hourglass, and its sensitivity depends upon the lattice geometries. Snap-through is a phenomenon in structural mechanics characterized by a sudden and rapid change in the configuration of a structure under load. It occurs when a structure undergoes a bifurcation point, transitioning from one stable equilibrium

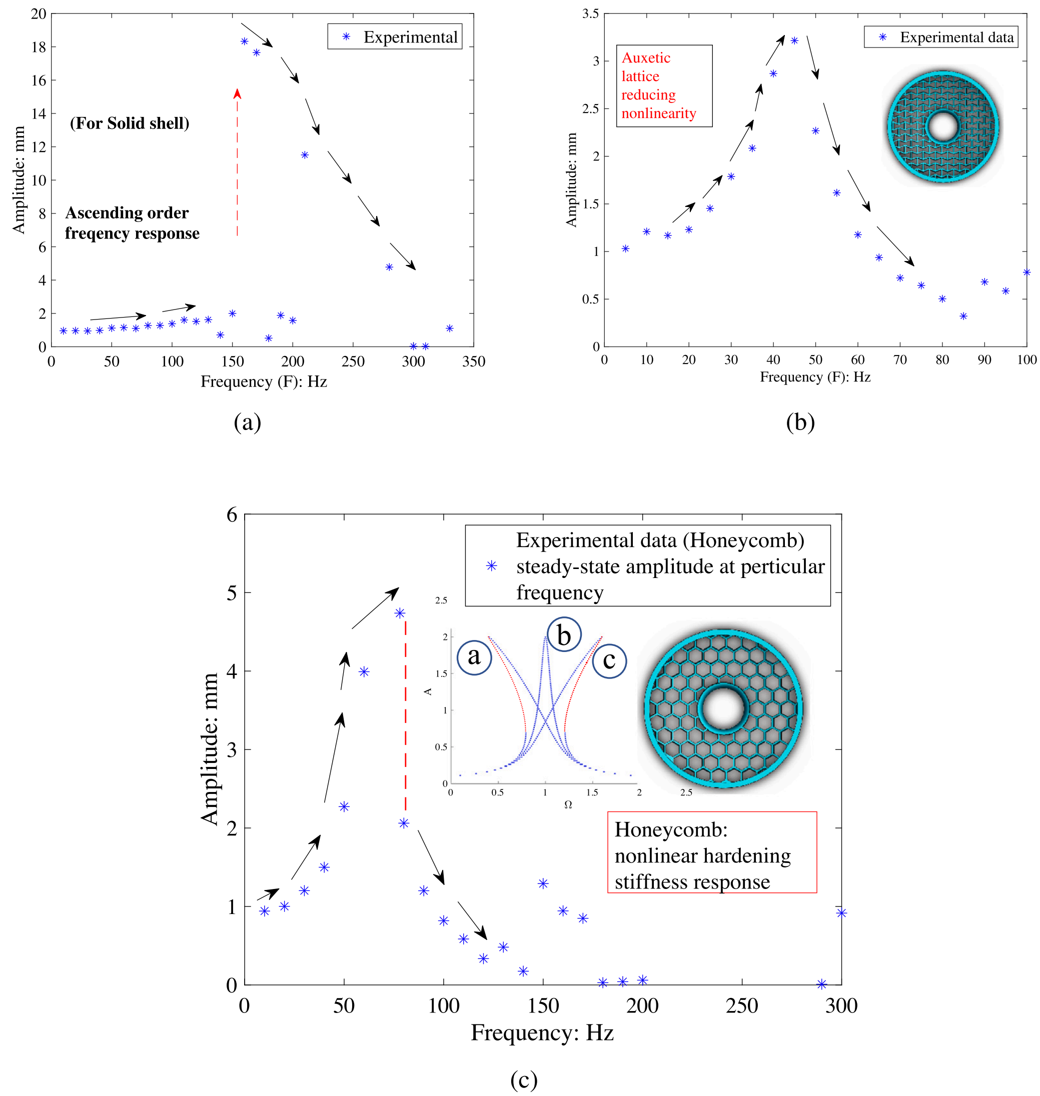

Fig. 5. These experimental plots show lattice based nonlinear effects on hourglass samples. The steady state harmonic response under different incremental frequencies have been collected through the laser Doppler vibrometer testings on these samples. It is observed that the solid shell (a) (without lattice) based hourglass metastructure normally gives softening type nonlinear stiffness profile, and this nonlinear profile becomes linear by providing auxetic lattice (b). Furthermore, the profiles become hardening type if the sample is based on honeycomb lattice (c).

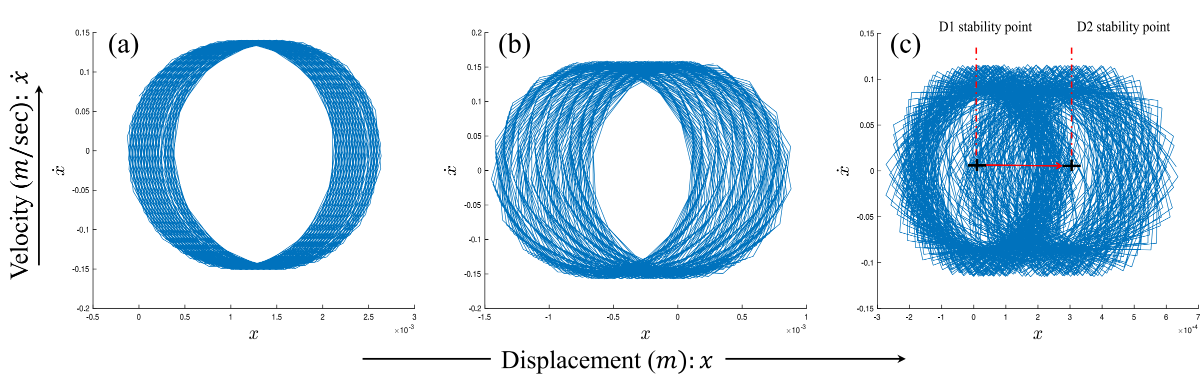

Fig. 6. Experimentally obtained phase portrait trajectories for nonlinear type hourglass 3D printed sample, shows displacement and velocity of the top plate that is x versus velocity, $\dot{x}$ (a) data points at lower frequencies show one equilibrium point, and the response is periodic in nature. (b) In-transition between one to two equilibrium points. (c) At higher frequencies shows two equilibrium centers separated from each other. The stable points D1 and D2 correspond to lower and upper domes, which are at (0,0) and (3,0), respectively.

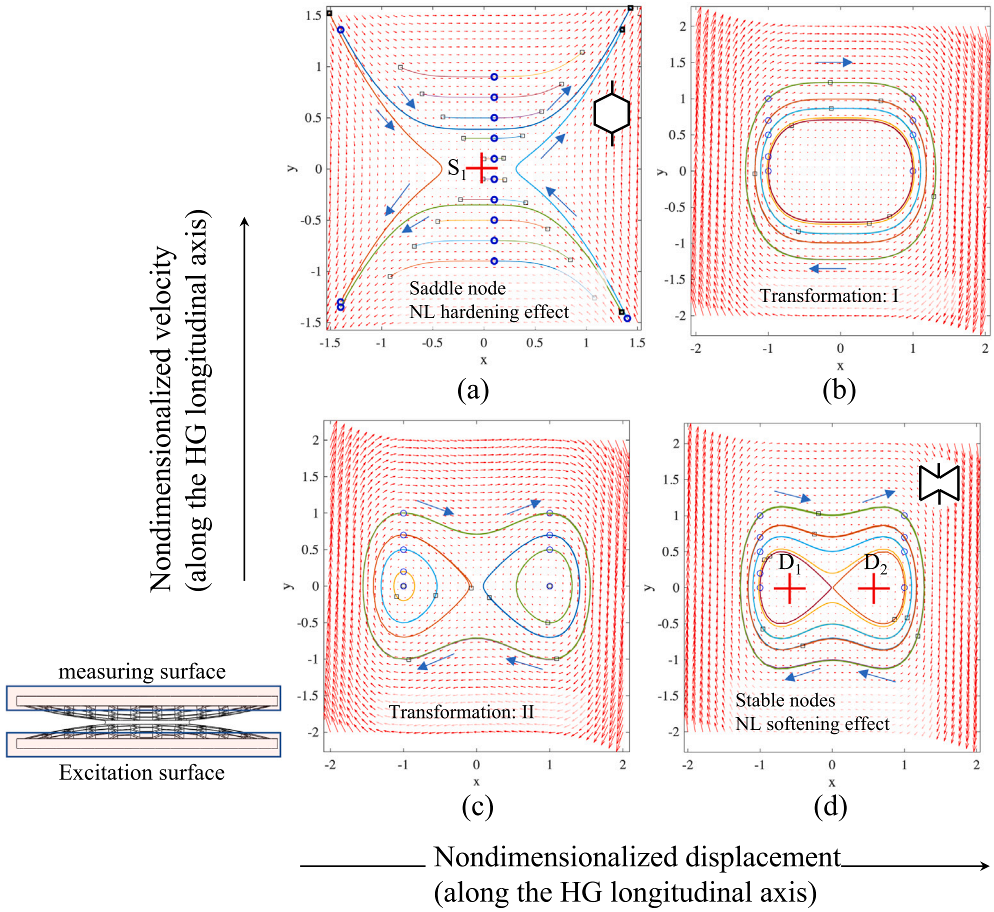

Fig. 7. Phase portraits were obtained using analytical formulations (see supplementary material) for three cases. (a) shows nondimensional normalized coordinates of displacement x versus velocity y parameters. The honeycomb-based hourglass sample shows a saddle–node pattern due to a nonlinear (NL) hardening case where the trajectories tend to meet at saddle point S_1 (0,0). (b,c) Show the transition effect from one to two equilibrium points due to nonlinear softening behavior from the solid shell-based hourglass to the auxetic cell-based hourglass. (d) It shows three fixed equilibrium nodes in which D_1 and D_2 are the stable nodes and the middle one at $(0,0)$ is the saddle–node for softening NL behavior due to the introduction of auxetic cells.

Table 1
Mechanical properties (PLA) used in simulation scheme, analysis and 3D printing specifications used to print the samples [38].

Properties	Values
Young's modulus of elasticity (E)	3.5 Gpa
Poisson's ratio (ν)	0.3
Density (ρ)	1.24 g/cm^3
Energy dissipation ratio (used in simulation)	0.1
3D printing parameters	
Material	PLA
Layer height thickness	0.15 mm
Infill density	100%
Infill pattern	Triangular

position to another through an unstable state. It can be exploited for desirable functionalities.

The test results show that the solid shell hourglass metastructure gives softening type of nonlinearity. The transitioning effect from nonlinear (softening) to linear response has been observed using the auxetic type of constituent cells. The snap-through effect is found to have disappeared while changing the metastructure from the solid shell to auxetic. On the other hand, the honeycomb cellular geometry causes to shift in response to hardening type nonlinearity, as shown in Figs. 5 and 6. It has been observed through the testing data that the phase portrait trajectories get separated from each other at higher frequencies. The phase plot are drawn in the vicinity of resonating frequency of corresponding samples. i.e. 100–200 Hz for solid shell, 30–60 Hz Auxetic, 50–200 Hz for honeycomb lattice.

In turn, it developed two stable equilibrium points at (0,0) and (3,0). The stable points $D1$ and $D2$ correspond to lower and upper domes. Phase portraits were obtained using analytical formulations (see supplementary information) for three cases. Fig. 7 shows nondimensional normalized coordinates of displacement x versus velocity y parameters. The honeycomb-based hourglass sample shows a saddle–node pattern due to nonlinear (NL) hardening case with the trajectories tend to meet at saddle point S_1 (0,0). The transition effect from one to two equilibrium points due to softening type nonlinear behavior from the solid shell-based hourglass to the auxetic cell-based hourglass has been observed as shown in Fig. 7b. Experimental observation of the phase plots matched well with the theoretical phase plots (see supplementary file for analytical calculations), showing similar trend for auxetic based hourglass sample. These are three fixed equilibrium nodes in which D_1 and D_2 are the stable nodes and the middle one at $(0,0)$ is the saddle–node for softening NL behavior due to introduction of auxetic cells as shown in Fig. 7c and d.

We have obtained phase portraits directly from the steady-state response at different frequencies under multiple gain values. The nonlinearity of the hourglass sample comes into picture at higher gain values under the specified (h/t) ratio, as shown in Fig. 5.

At higher frequencies, as the gain increases, the periodic solutions that are closed orbit move apart, as shown in Fig. 6. In turn, the fixed points also behave in a similar manner. It is found that each of the neutrally stable centers is surrounded by a family of closed orbits. The orbit, which has a small radius or is close to the fixed point, represents small oscillations about the equilibrium. The large orbit represents more energetic oscillations at higher frequencies. It can be anticipated from the phase plots that the large closed orbits encircle all the fixed points. It is also noted that the considered 3D printed structure has both material damping and lattice-based damping; therefore, the homoclinic orbits are absent in such kind of metastructures. With the help of experimental phase portrait trajectories, the stability of hourglass samples can be analyzed. For instance, the dynamic behavior of the double well obtained at higher frequencies is similar to that of the Duffing oscillators, as shown in Fig. 6. The higher energy orbits comprise two large circular trajectories with their centers located at $(0, 0)$ and $(3, 0)$ connected at $x = 1.5$, and represented by two families of circles. The load–deflection responses for a small value of the undeformed height of hourglass, H is non-linear and exponential, which is important for applications where the natural frequency of the system is required to be constant over a wide range of applied load [40,41].

4. Conclusions

We studied various nonlinear dynamic responses of 3D printed hourglass metastructure and its control using different combinations of cellular configurations. The tunable effect is generated by its constitutive cells ranging from auxetic to honeycomb geometries. Adaptive stiffness through the topology-controlled geometry can be exploited in lattice-based periodic metamaterials. The impact of cell design parameters on the resulting macroscopic behavior is assessed utilizing numerical simulations and experimental studies. The transition from softening to hardening nonlinear dynamic responses is reported with cell topologies ranging from the regular honeycomb and auxetic topologies that are widely used in fundamental cells. It has been observed from the numerical simulations that the honeycomb cell geometries give rise to hardening stiffness behavior. However, the auxetic gives rise to softening stiffness behavior. This characteristic has also been validated through the non-contact vibration measurement testing performed in different 3D printed hourglass samples using a laser Doppler vibrometer. Comparing the solid shell, auxetic, and honeycomb mechanical behavior of samples, it is observed that a transition happens from softening nonlinear response to linear response and then to hardening nonlinear response, respectively. The bistability phenomenon of the phase portraits discussed here offers unique opportunities for practical applications in medical contexts. For instance, in the design of implants or prosthetics, bistable hourglass metastructures can provide stable configurations that accommodate dynamic physiological changes, enhancing adaptability and functionality. Geometrical nonlinearities can have substantial mechanical effects, even if the constituent material behaves perfectly linearly. Its reversible nonlinear effects can be fine-tuned successfully by choosing the right combination of constitutive cells as details provided it the study. Furthermore, leveraging this bistability enables the development of innovative medical devices capable of responding dynamically to varying loads or movements within the body, showcasing the potential impact of nonlinear dynamics in healthcare technology. Our results and methods of investigation will be widespread application in understanding the mechanics of cellular-based structures such as foams, metamaterials [42,43], and bio-inspired cellular materials [23] such as porous geometry of bones in mechanobiology studies [44], etc. These materials are envisaged to be the future of lattice-based phononic crystals. In recent years, using electron microscope technology, micro and nano scale cellular structures such as honeycomb and auxetic have been developed and studied, which opens the door for cellular materials from engineering application to nano and biomedical fields.

CRediT authorship contribution statement

Vivek Gupta: Writing – review & editing, Writing – original draft, Validation, Software, Methodology, Investigation, Data curation, Conceptualization. **Sondipon Adhikari:** Writing – review & editing, Supervision, Project administration, Conceptualization. **Bishakh Bhattacharya:** Writing – review & editing, Supervision, Project administration, Conceptualization.

Declaration of competing interest

The authors declare that they have no known competing financial interests or personal relationships that could have appeared to influence the work reported in this paper.

Data availability

Data will be made available on request.

Acknowledgments

The authors gratefully acknowledges the grants received from "Scheme for Promotion of Academic and research collaboration" (SPARC) and Ministry of Human Resource Development, Govt. of India (MHRD) through grant number MHRD/ME/2018544 and the support of UK-India Education and Research Initiative (UKIERI), United Kingdom through grant number UKIERI/P1212.

Appendix A. Supplementary data

Supplementary material related to this article can be found online at https://doi.org/10.1016/j.mechrescom.2024.104261.

References

[1] L. Wu, Y. Wang, K. Chuang, F. Wu, Q. Wang, W. Lin, H. Jiang, A brief review of dynamic mechanical metamaterials for mechanical energy manipulation, Mater. Today 44 (2021) 168–193.
[2] H.N. Wadley, Multifunctional periodic cellular metals, Phil. Trans. R. Soc. A 364 (1838) (2006) 31–68.
[3] A.A. Zadpoor, Mechanical meta-materials, Mater. Horiz. 3 (5) (2016) 371–381.
[4] S. Bonfanti, R. Guerra, F. Font-Clos, D. Rayneau-Kirkhope, S. Zapperi, Automatic design of mechanical metamaterial actuators, Nature Commun. 11 (1) (2020) 1–10.
[5] Y. Prawoto, Seeing auxetic materials from the mechanics point of view: a structural review on the negative Poisson's ratio, Comput. Mater. Sci. 58 (2012) 140–153.
[6] M. Sanami, N. Ravirala, K. Alderson, A. Alderson, Auxetic materials for sports applications, Procedia Eng. 72 (2014) 453–458.
[7] X. Fei, L. Jin, X. Zhang, X. Li, M. Lu, Three-dimensional anti-chiral auxetic metamaterial with tunable phononic bandgap, Appl. Phys. Lett. 116 (2) (2020) 021902.
[8] H. Meng, W. Elmadih, H. Jiang, T. Lawrie, Y. Chen, D. Chronopoulos, Broadband vibration attenuation achieved by additively manufactured 3D rainbow hollow sphere foams, Appl. Phys. Lett. 119 (18) (2021) 181901.
[9] P. Celli, S. Gonella, Tunable directivity in metamaterials with reconfigurable cell symmetry, Appl. Phys. Lett. 106 (9) (2015) 091905.
[10] A. Nazir, K.M. Abate, A. Kumar, J.-Y. Jeng, A state-of-the-art review on types, design, optimization, and additive manufacturing of cellular structures, Int. J. Adv. Manuf. Technol. 104 (9) (2019) 3489–3510.
[11] V.S. Deshpande, N.A. Fleck, M.F. Ashby, Effective properties of the octet-truss lattice material, J. Mech. Phys. Solids 49 (8) (2001) 1747–1769.
[12] A. Vigliotti, D. Pasini, Stiffness and strength of tridimensional periodic lattices, Comput. Methods Appl. Mech. Engrg. 229 (2012) 27–43.
[13] P. Moongkhamklang, V. Deshpande, H. Wadley, The compressive and shear response of titanium matrix composite lattice structures, Acta Mater. 58 (8) (2010) 2822–2835.
[14] L.C. Geng, X.L. Ruan, W.W. Wu, R. Xia, D.N. Fang, Mechanical properties of selective laser sintering (SLS) additive manufactured chiral auxetic cylindrical stent, Exp. Mech. 59 (6) (2019) 913–925.

[15] R. Sala, S. Regondi, S. Graziosi, R. Pugliese, Insights into the printing parameters and characterization of thermoplastic polyurethane soft triply periodic minimal surface and honeycomb lattices for broadening material extrusion applicability, Addit. Manuf. (2022) 102976.
[16] D. Erdeniz, A.J. Levinson, K.W. Sharp, D.J. Rowenhorst, R.W. Fonda, D.C. Dunand, Pack aluminization synthesis of superalloy 3D woven and 3D braided structures, Metall. Mater. Trans. A 46 (1) (2015) 426–438.
[17] R. Gatt, L. Mizzi, J.I. Azzopardi, K.M. Azzopardi, D. Attard, A. Casha, J. Briffa, J.N. Grima, Hierarchical auxetic mechanical metamaterials, Sci. Rep. 5 (2015) 8395.
[18] D. Mousanezhad, S. Babaee, H. Ebrahimi, R. Ghosh, A.S. Hamouda, K. Bertoldi, A. Vaziri, Hierarchical honeycomb auxetic metamaterials, Sci. Rep. 5 (1) (2015) 1–8.
[19] B. Fotouhi, M.G. Rabbat, Dynamics of influence on hierarchical structures, Phys. Rev. E 88 (2) (2013) 022105.
[20] L.J. Gibson, Cellular solids, Mrs Bull. 28 (4) (2003) 270–274.
[21] N.A. Fleck, V.S. Deshpande, M.F. Ashby, Micro-architectured materials: past, present and future, Proc. R. Soc. A 466 (2121) (2010) 2495–2516.
[22] M. Miri, H. Stark, Persistent random walk in a honeycomb structure: Light transport in foams, Phys. Rev. E 68 (3) (2003) 031102.
[23] D. Goss, C.A. Penick, A. Grishin, D. Bhate, Bio-inspired design and additive manufacturing of cellular materials, in: Biomimicry for Aerospace, Elsevier, 2022, pp. 141–185.
[24] M.F. Ashby, The properties of foams and lattices, Phil. Trans. R. Soc. A 364 (1838) (2006) 15–30.
[25] R. Lakes, Deformation mechanisms in negative Poisson's ratio materials: structural aspects, J. Mater. Sci. 26 (9) (1991) 2287–2292.
[26] K.E. Evans, Auxetic polymers: a new range of materials, Endeavour 15 (4) (1991) 170–174.
[27] S. Belouettar, A. Abbadi, Z. Azari, R. Belouettar, P. Freres, Experimental investigation of static and fatigue behaviour of composites honeycomb materials using four point bending tests, Compos. Struct. 87 (3) (2009) 265–273.
[28] J. Zhang, G. Lu, Z. You, Large deformation and energy absorption of additively manufactured auxetic materials and structures: A review, Composites B (2020) 108340.
[29] R. Lakes, Foam structures with a negative Poisson's ratio, Science 235 (1987) 1038–1041.
[30] S. Chen, K.C. Chan, F. Wu, L. Xia, Pronounced energy absorption capacity of cellular bulk metallic glasses, Appl. Phys. Lett. 104 (11) (2014) 111907.
[31] P. Eghbali, D. Younesian, S. Farhangdoust, Enhancement of the low-frequency acoustic energy harvesting with auxetic resonators, Appl. Energy 270 (2020) 115217.
[32] C. Luo, C.Z. Han, X.Y. Zhang, X.G. Zhang, X. Ren, Y.M. Xie, Design, manufacturing and applications of auxetic tubular structures: A review, Thin-Walled Struct. 163 (2021) 107682.
[33] C. Pan, Y. Han, J. Lu, Design and optimization of lattice structures: A review, Appl. Sci. 10 (18) (2020) 6374.
[34] S.H. Kang, S. Shan, A. Košmrlj, W.L. Noorduin, S. Shian, J.C. Weaver, D.R. Clarke, K. Bertoldi, Complex ordered patterns in mechanical instability induced geometrically frustrated triangular cellular structures, Phys. Rev. Lett. 112 (9) (2014) 098701.
[35] P. Wang, F. Casadei, S. Shan, J.C. Weaver, K. Bertoldi, Harnessing buckling to design tunable locally resonant acoustic metamaterials, Phys. Rev. Lett. 113 (1) (2014) 014301.
[36] J.T. Overvelde, K. Bertoldi, Relating pore shape to the non-linear response of periodic elastomeric structures, J. Mech. Phys. Solids 64 (2014) 351–366.
[37] G.W. Milton, Complete characterization of the macroscopic deformations of periodic unimode metamaterials of rigid bars and pivots, J. Mech. Phys. Solids 61 (7) (2013) 1543–1560.
[38] V. Gupta, S. Adhikari, B. Bhattacharya, Exploring the dynamics of hourglass shaped lattice metastructures, Sci. Rep. 10 (1) (2020) 1–12.
[39] V. Gupta, B. Bhattacharya, S. Adhikari, Energy absorption of hourglass shaped lattice metastructures, Exp. Mech. (2022) 1–10.
[40] J.P. Den Hartog, Mechanical Vibrations, Courier Corporation, 1985.
[41] C.M. Harris, A.G. Piersol, Harris' Shock and Vibration Handbook, Vol. 5, McGraw-Hill New York, 2002.
[42] V. Gupta, R.K. Munian, B. Bhattacharya, Dispersion analysis of the hourglass-shaped periodic shell lattice structure, Int. J. Solids Struct. (2022) 111931.
[43] H. Mirani, V. Gupta, S. Adhikari, B. Bhattacharya, Tailoring of interface modes in topologically protected edge states with hourglass lattice metamaterials, J. Sound Vib. 562 (2023) 117814.
[44] A. Gryko, P. Prochor, E. Sajewicz, Finite element analysis of the influence of porosity and pore geometry on mechanical properties of orthopaedic scaffolds, J. Mech. Behav. Biomed. Mater. (2022) 105275.